Received: 9 July 2024 | Revised: 7 October 2024 | Accepted: 15 October 2024

DOI: 10.1096/fj.202401565RR

RESEARCH ARTICLE

The FASEB Journal

Angiotensin-(1–7) improves intestinal microbiota disturbances and modulates fecal metabolic aberrations in acute pancreatitis

Ruru Gu[1,2] | **Hongtao Wei**[3] | **Tianyu Cui**[1] | **Guoxing Wang**[4] | **Yingyi Luan**[1] | **Ruixia Liu**[1] | **Chenghong Yin**[1]

[1]Central Laboratory, Beijing Obstetrics and Gynecology Hospital, Beijing Maternal and Child Health Care Hospital, Capital Medical University, Beijing, China

[2]Department of Gastroenterology, the Second Hospital of Shandong University, Jinan, China

[3]Department of Gastroenterology, Beijing Friendship Hospital, Capital Medical University, Beijing, China

[4]Department of Emergency Medicine, Beijing Friendship Hospital, Capital Medical University, Beijing, China

Correspondence

Ruixia Liu and Chenghong Yin, Central Laboratory, Beijing Obstetrics and Gynecology Hospital, Beijing Maternal and Child Health Care Hospital, Capital Medical University, Beijing, China.
Email: liuruixia@ccmu.edu.cni and yinchh@ccmu.edu.cn

Abstract

Acute pancreatitis (AP) is a serious health problem that dysregulates intestinal microbiota. Angiotensin (Ang)-(1–7) plays a protective role in the intestinal barrier in AP, but its effect on intestinal microbiota remains clear. To investigate the impact of Ang-(1–7) on AP-induced intestinal microbiota disorder and metabolites. We collected blood and fecal samples from 31 AP patients within 48 h after admission to the hospital, including 11 with mild AP (MAP), 14 with moderately severe AP (MSAP), six with severe AP (SAP). Mice were divided into four groups: control, AP, AP + Ang-(1–7) via tail vein injection, and AP + Ang-(1–7) via oral administration. The samples of mice were collected 12 h after AP. Pancreatic and intestinal histopathology scores were analyzed using the Schmidt and Chiu scores. Fecal microbiota and metabolites analysis was performed via 16S rDNA sequencing and nontargeted metabolomics analysis, respectively. In patients, the abundance of beneficial bacteria (*Negativicutes*) decreased and pathogenic bacteria (*Clostridium bolteae and Ruminococcus gnavus*) increased in SAP compared with MAP. Ang-(1–7) levels were associated with changes in the microbiota. There were differences in the intestinal microbiota between control and AP mice. Ang-(1–7) attenuated intestinal microbiota dysbiosis in AP mice, reflecting in the increase in beneficial bacteria (*Odoribacter and Butyricimonas*) than AP, as well as pancreatic and intestinal injuries. Oral administration of Ang-(1–7) reversing AP-induced decreases in metabolisms: secondary bile acids, emodin, and naringenin. Ang-(1–7) may improve intestinal microbiota dysbiosis and modulate fecal metabolites in AP, thereby reducing the damage of AP.

KEYWORDS

acute pancreatitis, angiotensin-(1–7), intestinal microbiota, metabolites

ABBREVIATIONS: AMY, amylase; Ang-(1–7), Angiotensin-(1–7); AP, acute pancreatitis; CAE, caerulein; CECT, contrast-enhanced computed 107 tomography; DAO, diamine oxidase; D-lac, D-lactate; HE, hematoxylin and eosin; LPS, lipopolysaccharide; MAP, mild acute pancreatitis; MRI, magnetic resonance imaging; MSAP, moderately severe acute pancreatitis; SAP, severe acute pancreatitis; SCFAs, short-chain fatty acids.

Ruru Gu and Hongtao Wei contributed equally to this work and share first authorship.

1 | INTRODUCTION

Acute pancreatitis (AP) is an acute abdominal disorder in clinical settings the morbidity of which is increasing worldwide.[1] Severe acute pancreatitis (SAP) occurs in about 20% of AP patients. SAP is characterized by acute development, severe complications, and a fatality rate of 20–40%.[2] Intestinal injury is well recognized as an early serious complication of AP, which can cause multiple organ infections and aggravate the condition.[3,4] However, the pathogenesis of intestinal dysfunction and infection complications remains unclear.

Intestinal injury has been found linked with poor outcomes in AP patients.[5] Several studies have detected alterations of the intestinal microbiota in AP patients and animals. The disordered intestinal microbiota in AP includes a decrease in beneficial bacteria such as *Bifidobacterium* and an increase in pathogenic bacteria such as *Escherichia–Shigella*.[6] The imbalance of intestinal flora destroys the biological barrier and increases intestinal permeability, which provides a pathway for pathogens to migrate and eventually leads to organ infections.[6,7] The treatment for intestinal flora disorder focuses on the probiotics. However, the multispecies probiotic preparation increases intestinal injuries and bacterial translocation in AP patients with organ failure.[8] Therefore, it is significant to explore the changes in intestinal microbiota during AP and find targeted treatments for specific bacteria.

Angiotensin (Ang)-(1–7) is a member of the ACE2/Ang-(1–7)/Mas receptor axis.[9] Ang-(1–7) delivered orally via probiotic increases the content of *Lactobacillus paracasei* and A*kkermansia muciniphila* in older rats.[10] Oral Ang-(1–7) peptide decreases the gDNA expression of *Enterobacter cloacae* in high-fat diet mice.[11] Our previous studies have found that Ang-(1–7) improves pancreatic injuries and intestinal barrier dysfunction in AP.[12,13] Thus, we speculated that Ang-(1–7) may ameliorate AP injuries by improving intestinal microbiota dysbiosis.

In this study, we explored the changes in intestinal microbiota in patients during the progression of AP. We used AP mice to investigate the effects of AP on intestinal microbiota and further explore the function of Ang-(1–7) in intestinal microbiota by 16S rDNA gene sequencing. The fecal metabolites in AP mice and the impact of Ang-(1–7) were analyzed by nontargeted metabolomics analysis as well.

2 | MATERIALS AND METHODS

2.1 | Patients' recruitment and study design

From the Department of Emergency of the Beijing Friendship Hospital, Capital Medical University, China, a total of 49 AP patients aged over 18 presenting were registered within 7 days of the onset of AP disease. All patients were in line with the 2012 AP classification of Atlanta,[14] requiring two of the following three features: (1) abdominal pain consistent with acute pancreatitis (acute onset of a persistent, severe, epigastric pain often radiating to the back); (2) serum lipase activity (or amylase activity) at least three times greater than the upper limit of normal; and (3) characteristic findings of acute pancreatitis on contrast-enhanced computed tomography (CECT) and less commonly magnetic resonance imaging (MRI) or transabdominal ultrasonography. The following patients who satisfied the following criteria were excluded including (1) chronic pancreatitis; (2) metabolic disorder, gastrointestinal, liver, immunodeficiency diseases; (3) malignant cancer; (4) a long history of taking immunosuppressants, hormones, antibiotics, and other special drugs; (5) lack of information or samples. In this study, 31 AP patients were included in the final analysis. According to clinical severity, patients were divided into three groups: MAP, MSAP, and SAP.[14] Every participant signed a written informed consent. Demographics and clinical variables were collected during the hospitalization.

2.2 | Samples collection and measurement of AP patients

The blood and fecal samples from patients were received within 48 h after admission to the hospital. Fecal samples were collected in the stool tube containing stool preservation liquid (Shanghai Realbio Technology Co., China) after AP patients urinated. Fecal samples were transported to the hospital on the day they were collected and stored at −80°C until analysis. Blood samples were centrifuged at 3000 rpm for 15 min to acquire the serum samples, which were saved in −80°C until needed for assays. Serum amylase (AMY) was measured with commercial kits (Nanjing Jiancheng Institute of Biotechnology, Nanjing, China). Serum Ang-(1–7) was measured with an ELISA kit (Cloud, Wuhan, China). Gut barrier permeability was assessed by detecting serum diamine oxidase (DAO) and D-lactate (D-lac) by commercial kits (Abcam, Cambridge, UK for D-lac and Nanjing Jiancheng Institute of Biotechnology for DAO).

2.3 | Animal experiments

Six-week-old male C57BL/6 mice (body weight 20–22 g) were obtained from Beijing Vital River Laboratory Animal Technologies Co. Ltd. (Beijing, China). The caerulein (CAE) plus lipopolysaccharide (LPS)-induced AP model

was established as previously described (CAE, 100 μg/kg intraperitoneally six times and 10 mg/kg LPS intraperitoneally once).[12] Control mice were given the same volume of normal saline instead of CAE and LPS. The mice in the Ang IV group and Ang IG group received 500 μg/kg Ang-(1–7) analog through tail vein injection or oral administration immediately after the LPS injection, respectively.

2.4 | Samples collection of AP mice

The mice from each group were anesthetized (induced with carbon dioxide for 15 s in an airtight container) 12 h after AP induction. Fecal samples were collected by sterile tools and saved in −80°C for further analysis. Pancreatic and intestinal tissues were harvested; a subset of tissues was immediately fixed in 4% paraformaldehyde.

2.5 | Histopathological analysis

Fresh pancreatic and distal ileal segments were fixed in 4% paraformaldehyde overnight, dehydrated in ethanol gradients, and embedded in paraffin blocks. Tissues were sectioned into 5 μm layers and stained with hematoxylin and eosin (HE).

Histopathologic damage in the pancreas tissues during AP was evaluated according to Schmidt's score.[15] Chiu's score represents injuries to intestinal tissues in AP.[16] Histopathological scores were determined by the independent assessment of three distinct regions of the pancreas or intestine.

2.6 | 16S rDNA gene sequencing

According to the manufacturer's instructions, total genomic DNA was extracted by the sodium dodecyl sulfate and cetyltrimethyl ammonium bromide methods. The following primers were used to amplify the highly variable V3-V4 regions of the bacterial 16S rDNA genes: 341F (5′-CCTAYGGGRBGCASCAG-3′) and 806R (5′-GGACTACNNGGGTATCTAAT-3′). The following substances are required for the PCR reactions: 0.2 μM of forward and reverse primers, 15 μL of Phusion® High-Fidelity PCR Master Mix (New England Biolabs), and about 10 ng of template DNA. The following conditions are required for the PCR reactions: the end cycle consisted of initial denaturation at 98°C for 1 min, then denaturation for 10s at 98°C, annealing for 30s at 50°C, extension for 30 s at 72°C, and lastly elongation for 5 min at 72°C. PCR products were detected by electrophoresis on 2% agarose gels. PCR products were evenly mixed in proportion and purified with the Qiagen Gel Extraction Kit (Qiagen, Germany). Sequencing libraries were established by the TruSeq® DNA PCR-Free Sample Preparation Kit (Illumina, USA), with adding the index code. The quality of library was evaluated with a Qubit@ 2.0 Fluorometer (Thermo Fisher Scientific, USA) and an Agilent Bioanalyzer 2100 system. On an Illumina NovaSeq platform, the library was sequenced, producing 250 bp paired-end reads.

2.7 | Fecal metabolic profiles analysis

One hundred milligrams of stool sample was mixed with 400 μL of extract containing isotope-labeled internal standard mixture (acetonitrile: methanol = 1: 1) in a test tube. After 30 s of vortex, the samples were sonicated in an ice-water bath for 5 min. The samples were then incubated for 1 h at −40°C and centrifuged at 12 000 rpm for 15 min at 4°C. Four hundred microliters of supernatant was transferred to a new test tube and dried in a 37°C vacuum concentrator.

The dried sample was sonicated on ice for 10 min with 200 μL 50% acetonitrile, then centrifuged at 13 000 rpm for 15 min at 4°C. Seventy-five microliters of supernatant was transferred to a new glass bottle for LC/MS analysis. The quality control samples were prepared by mixing equal amounts of supernatant.

For UHPLC separation, the ExionLC Infinite series UHPLC system was used (AB Sciex, Boston, MA, USA), with a UPLC BEH Amide column (2.1 × 100 mm, 1.7 μm, Waters). The mobile phase concluded 25 mmol/L ammonium acetate and 25 mmol/L ammonia hydroxide dissolved in water (pH = 9.75) (A) and acetonitrile (B). The following elution gradients were used in the analysis: 0–0.5 min, 95% B; 0.5–7.0 min, 95%–65% B; 7.0–8.0 min, 65%–40% B; 8.0–9.0 min, 40% B; 9.0–9.1 min, 40%–95% B; 9.1–12.0 min, 95% B. The column temperature was 25°C. During an LC/MS experiment, MS/MS spectra were acquired using the TripleTOF 5600 mass spectrometry (AB Sciex) on an information-dependent basis mode. According to the preselection criteria, the acquisition software (Analyst TF 1.7, AB Sciex) incessantly assessed the full sweep measurement MS data when collecting and triggering the MS/MS spectra. In each cycle, 12 precursor ions with an intensity greater than 100 were selected for MS/MS when the impact energy was 30 eV. The cycle time was 0.56 s. The following ESI source conditions were set in the operation: Gas 1 as 60 psi, Gas 2 as 60 psi, Curtain Gas as 35 psi, Source Temperature as 600°C, Declustering potential as 60 V, Ion Spray Voltage Floating as 5000 or −4000 V in positive or negative modes, respectively.

2.8 | Statistical analysis

Data are shown as mean ± SD. Statistical analyses were carried out using SPSS 22.0 (IBM, USA). For the comparison of normally continuous variables, the Wilcoxon rank sum test was used. For the comparison of non-normally continuous variables, a Student's *t*-test was used. Statistical significances of multiple comparisons were corrected by Benjamini–Hochberg false discovery rate (FDR), and significant association was considered below an FDR threshold of 0.05.

2.9 | Ethics statement

The study of patients was conducted in accordance with the Declaration of Helsinki, and approved by the Ethics Committee of Beijing Friendship Hospital (protocol code: 2022-P2-010-01). The study of animals was approved by the Animal Experimental Committee of Capital Medical University (protocol code: AEEI-2022-125).

3 | RESULTS

3.1 | Clinical characteristics of AP patients

A total of 31 AP patients were enrolled from September 2021 to January 2022, including 11 with MAP, 14 with MSAP, and six with SAP. The demographic and clinical characteristics of AP patients are shown in Table 1. There were no differences in age and gender among MAP, MSAP, and SAP, indicating comparability among the three groups. The gastrointestinal function scores increased significantly with the progression of the AP disease (The score criteria are shown in Table S1). The incidences of infection complications and multiple organ failure in SAP were higher than those in MSAP and MAP. The length of hospital stays did not differ among the three groups. The serum levels of Ang-(1–7), DAO, and D-lac increased with the deterioration of AP, but there was no statistical significance.

3.2 | Gut microbial diversity in AP patients

Among the 31 fecal samples, sequence denoising, pruning, and chimera selection resulted in a final analysis of 1 455 768 reads. These reads were clustered into 358 OTUs. The rarefaction and Shannon curves showed that most samples tended to be flat, which indicated that the sequencing covered the biodiversity (Figure S1).

Subsequently, we used four α-diversity indices to assess the abundance and diversity of the microbiota, that is, abundance-based coverage estimator (ACE), Shannon, Chao1, and Simpson. The results from the four α-diversity indices exhibited no difference across the diverse groups (Figure 1A–D).

Next, we evaluated the β-diversity of microbiota among groups by the unweighted principal coordinate analysis (PCoA) and unweighted distance matrices (nonmetric multidimensional scaling [NMDS]). Although the MAP group could not be separated entirely from the MSAP and SAP groups, the distribution is slightly different from the two groups, which indicates that the severity of AP affected the intestinal microbiota of patients (Figure 1E,F). Furthermore,

TABLE 1 Demographic and clinical characteristics of the study participants.

	MAP ($n=11$)	MSAP ($n=14$)	SAP ($n=6$)	*p* value
Age, years	67 (34–86)	68 (35–86)	71 (48–85)	.610
Sex, male/female	5/6	6/8	3/3	
AMY, U/L	110.54 (28.63–199.60)	174.55 (85.09–319.68)	187.28 (28.63–311.73)	.585
Ang-(1–7), pg/mL	127.16 (40.25–184.10)	134.28 (23.11–818.61)	142.21 (33.47–141.37)	.971
D-lac, nmol/mL	7.19 (3.38–24.14)	14.89 (1.65–30.95)	12.33 (8.73–17.84)	.474
DAO, ng/mL	2.44 (0.35–108.95)	3.32 (0.00–95.33)	2.79 (0.00–9.08)	.971
BISAP, 24 h	1.0 (1–3)	1.5 (0–3)	2.5 (2–4)	.012
APACHE II, 24 h	4.0 (1–5)	5.5 (0–9)	7.5 (5–9)	.006
Gastrointestinal function scores, 24 h	0.0 (0–1)	1.0 (0–2)	1.5 (1–2)	.009
Infection complications (%)	0	35.7	66.7	.018
Multiple organ failure (%)	0	0	66.7	<.001
Hospital stay, days	9 (7–15)	11.5 (5–20)	11.5 (8–14)	.315

Abbreviations: AMY, amylase; Ang-(1–7), Angiotensin-(1–7); DAO, diamine oxidase; D-lac, D-lactate; MAP, mild acute pancreatitis; MSAP, moderately severe acute pancreatitis; SAP, severe acute pancreatitis.

the Permanova/Anosim analysis showed no obvious difference in β diversity among the three groups (Figure 1G).

3.3 | Taxonomic characterization of the intestinal microbial profiles across AP severity in patients

Next, we described the alterations of intestinal microbiota in patients during AP progression. The linear discriminant analysis effect size (LEfSe) characterized that the abundance of *Negativicutes* increased in MAP compared to MSAP and SAP. The LEfSe also revealed significant increases of *Lachnoclostridium*, *Clostridium bolteae, and Ruminococcus gnavus* in SAP than those in MAP and MSAP (Figure 2A,B).

By investigating the resemblance of bacterial classification at the phylum and genus level, the general structure of intestinal microbiota in the three groups was further compared. At the phylum level, *Bacteroidetes, Firmicutes,* and *Proteobacteria* were the main phyla (Figure 2C). At the genus level, the *Bacteroides, Escherichia–Shigella, Akkermansia, Enterococcus, Klebsiella*, and *Parabacteroides* were dominant genera (Figure 2D). Spearman correlation analysis was performed on intestinal bacteria and related indexes in AP patients. Figure 2E shows a significant negative correlation between serum Ang-(1–7) levels and *Negativicutes* ($r = -.376$, $p = .037$). Meanwhile, Figure 2F shows a significant positive correlation between the gastrointestinal function scores and *R. gnavus* ($r = .405$, $p = .024$). It suggested that intestinal microbiota dysbiosis is associated with AP severity and gastrointestinal injury. These bacteria (*Negativicutes and R. gnavus*) can be targeted and regulated in AP, which deserves further study.

3.4 | Ang-(1–7) attenuated pancreatic and intestinal injuries in AP mice

Mouse AP models were successfully established using CAE and LPS. There was no obvious inflammatory phenotype in the pancreas of the control mice. However, the AP mice showed interlobular edema, hemorrhage, and inflammatory cell infiltration. Ang-(1–7) therapy diminished the pancreatic injuries induced by AP (Figure 3A). Pancreatic pathological scores were considerably higher in the AP group compared to the control group (Figure 3B, $p < .01$). Furthermore, in comparison with the AP group, both the Ang IV and Ang IG groups had diminished pathological damage and displayed lower overall scores (Figure 3B, $p < .01$). In the AP mice, the intestinal mucosa was necrotic and exfoliated, villi were ruptured, and higher levels of inflammatory cell infiltration were detected relative to those in the control group (Figure 3C). As shown in Figure 3C, Ang-(1–7) administration considerably protected against and diminished AP-related intestinal injuries. Chiu's score indicated that the extent of damage to the intestinal mucosa in AP mice was more severe than that in the control group (Figure 3D, $p < .01$). The incremental Chiu's score in AP mice was significantly reversed by Ang-(1–7) compared to the AP group (Ang IV vs. AP: $p < .05$; Ang IG vs. AP: $p < .05$; Figure 3D).

3.5 | Ang-(1–7) reversed gut microbiota dysbiosis in AP mice

Because Ang-(1–7) is protective against intestinal injury, we used fecal samples for 16S rDNA sequencing to explore the influence of Ang-(1–7) on the intestinal microbiota in AP mice. From 34 fecal samples, we obtained the full length of bacteria. The coverage and Shannon curves showed that most samples tended to be flat (Figure S2), which suggested that the volume of sequencing data was reasonable and sufficient. Subsequently, we used four α-diversity indices to measure the abundance and diversity of the microbiota, that is, ACE, Shannon, Simpson, and Chao1. There were no differences in the four α-diversity indices among the four groups (Figure 4A–D), which demonstrated that the α-diversity of intestinal microbiota is not altered by AP or Ang-(1–7) treatment.

Next, we evaluated the β-diversity of gut microbiota among groups by the PCoA and NMDS. Although the CON group could not be separated entirely from the AP group, the distribution is slightly different from the AP group (Figure 4E,F). The Ang-(1–7) IG group was mostly separated from the AP group, while the distribution of the Ang IV was slightly dissimilar to the AP group, demonstrating that Ang-(1–7) changes the intestinal microbial structure of the AP mice (Figure 4E,F). The PCoA and NMDS results showed that the general intestinal microbial profiles were different across the four groups (Figure 4E,F). Furthermore, the Permanova/Anosim analysis showed no obvious difference in β diversity among the four groups (Figure 4G).

To determine the key intestinal microbiota considerably changed by AP or Ang-(1–7) treatment, all sequences were analyzed with the LEfSe method. In the CON group, the characteristics of microbiota were concentrated in the genus *Ruminococcus and Oscillospira*, the family *Lachnospiraceae and Ruminococcaceae,* the phylum *Firmicutes* (Figure 5). The intestinal microbiota of the AP group was characterized by the enrichment of the genus *Dehalobacterium* and the family *Dehalobacteriaceae* (Figure 5). The *Odoribacter* and *Sutterella* genus was enriched in the Ang-(1–7) IG group, whereas the *Odoribacteraceae* and *Butyricimonas* genus were enriched

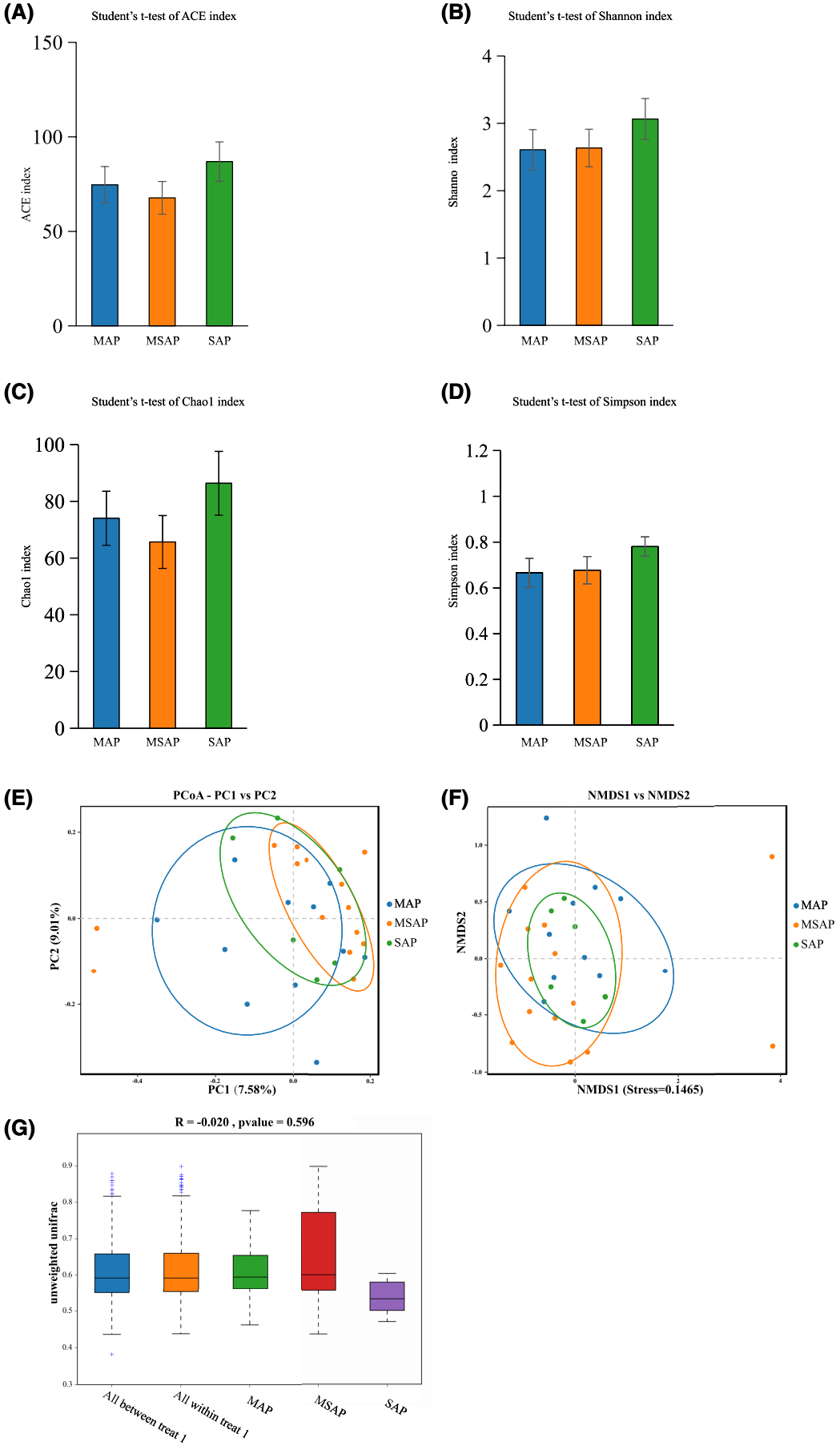

FIGURE 1 The effects of AP severity on alpha and beta diversity of gut microbiota. Analysis of gut microbial diversity was performed on the basis of 16S rDNA sequencing. (A) ACE index. (B) Shannon index. (C) Chao1 index. (D) Simpson index. Bacterial community compositional similarity was evaluated by beta diversity. Plots of unweighted UniFrac-based PCoA (E) and nonmetric multidimensional scaling (NMDS) plots based on Jaccard dissimilarity (F) are presented. Analysis of similarities (Anosim) was used to detect differences between the groups (G).

in the Ang-(1–7) IV group (Figure 5), which revealed that Ang-(1–7) could restructure the microbial composition of the intestine in AP mice.

3.6 | Ang-(1–7) modulated fecal metabolites in AP mice

The fecal metabolites in the four groups were determined by nontargeted metabolomics, revealing the effect of Ang-(1–7) on fecal metabolites in AP mice. The principal component analysis presented that the main metabolic profiles were different among the four groups (Figure 6A). The supervised orthogonal projections to latent structures-discriminant analysis score plot also displayed the apparent separations between the AP and Ang-(1–7) IV group, and between the AP and Ang-(1–7) IG group (Figure 6C,D).

The relative abundances of over 200 metabolites in the CON and AP groups changed in the volcano plot (Figure 6E), which revealed that the contents of most of the fecal metabolites in AP mice were different from those of CON mice, suggesting AP has a significant effect on fecal metabolic profiles. Ang-(1–7) treatment also dramatically altered the abundance of fecal metabolites compared with AP mice (Figure 6F,G).

The heat maps showed that the abundances of emodin, naringenin, deoxycholic acid, etc. were decreased by AP inducing compared with CON group (Figures S3 and S4). The heat maps showed the opposite trends after Ang-(1–7) administration in AP mice, such as Ang IG that increased the abundances of emodin, naringenin, and deoxycholic acid (Figure 7A,B). In particular, the alterations in the abundances of bile acids caused by AP stimulation were obviously enlarged by Ang-(1–7) treatment. For example, the abundances of deoxycholic acid and isolithocholic acid were increased in the Ang IV group compared with the AP group (Figure 7C,D). The abundances of deoxycholic acid, ursodeoxycholic acid, chenodeoxycholic acid, and isohyodeoxycholic acid were increased in the Ang IG group compared with the AP group (Figure 7E–H). The differential abundance score (DA Score) illustrated the upregulated pathways of overall expression in Ang IG mice than these in AP mice, such as bile secretion, regulation of lipolysis in adipocytes, arachidonic acid metabolism, and ABC transporters (Figure S5).

4 | DISCUSSION

This study found that AP was correlated with dysregulation of the intestinal microbiota which was associated with inflammation and intestinal barrier dysfunction. The contents of the intestinal microbiota in SAP patients varied from MAP and MSAP, which suggests its involvement in the deterioration of AP. For the first time, we revealed the effects of Ang-(1–7) in intestinal microbiota and metabolism in AP mice.

First of all, a total of 31 AP patients were enrolled in this study, including 11 with MAP, 14 with MSAP, and six with SAP. A recent study recruited 20 patients diagnosed with AP and categorized them by severity (7 SAP and 13 MAP).[17] In another study, 20 patients with SAP were divided into two groups: 10 in the intra-abdominal infected group and 10 in the noninfected group.[18] Thus, we thought that the selection of six SAP is acceptable. We discovered that the contents of the intestinal microbiota in SAP patients varied from MAP and MSAP, which indicated the connection between microbial dysregulation and AP severity. Intestinal dysfunction often occurs at the early stage of AP, which may account for the acceleration of AP progression and its deterioration into SAP.[19] The intestinal barriers are commonly classified into four types: mechanical barrier, chemical barrier, immune barrier, and biological barrier (intestinal microbiota).[6] At the early stage of AP, the normal microbiome environment can be converted into a pathogenic state called microbial imbalance. After the intestinal barrier is compromised, disordered microbiota translocate through the gut to distal organs, causing infection, exacerbating disease, and even death.[6] In AP patients with different severity classifications, there were dissimilar distributions of intestinal microbiota. The LEfSe revealed that the abundance of *Negativicutes* was increased in AP compared to MSAP and SAP. Dai et al. reported that 6-methoxybenzoxazolinone upregulates the content of *Negativicutes* to produce acetate and propionate in the cecum of voles.[20] The class *Negativicutes* includes *Selenomonadales*, which has been confirmed to ferment carbohydrates into acetate.[21] Short-chain fatty acids (SCFAs) include acetate, propionate, and butyrate, which are not only a vital energy source for colon epithelial cells but also inhibit the release of pro-inflammatory cytokines and increase the production of tight junction proteins to maintain the intestinal barrier.[22–24] The LEfSe

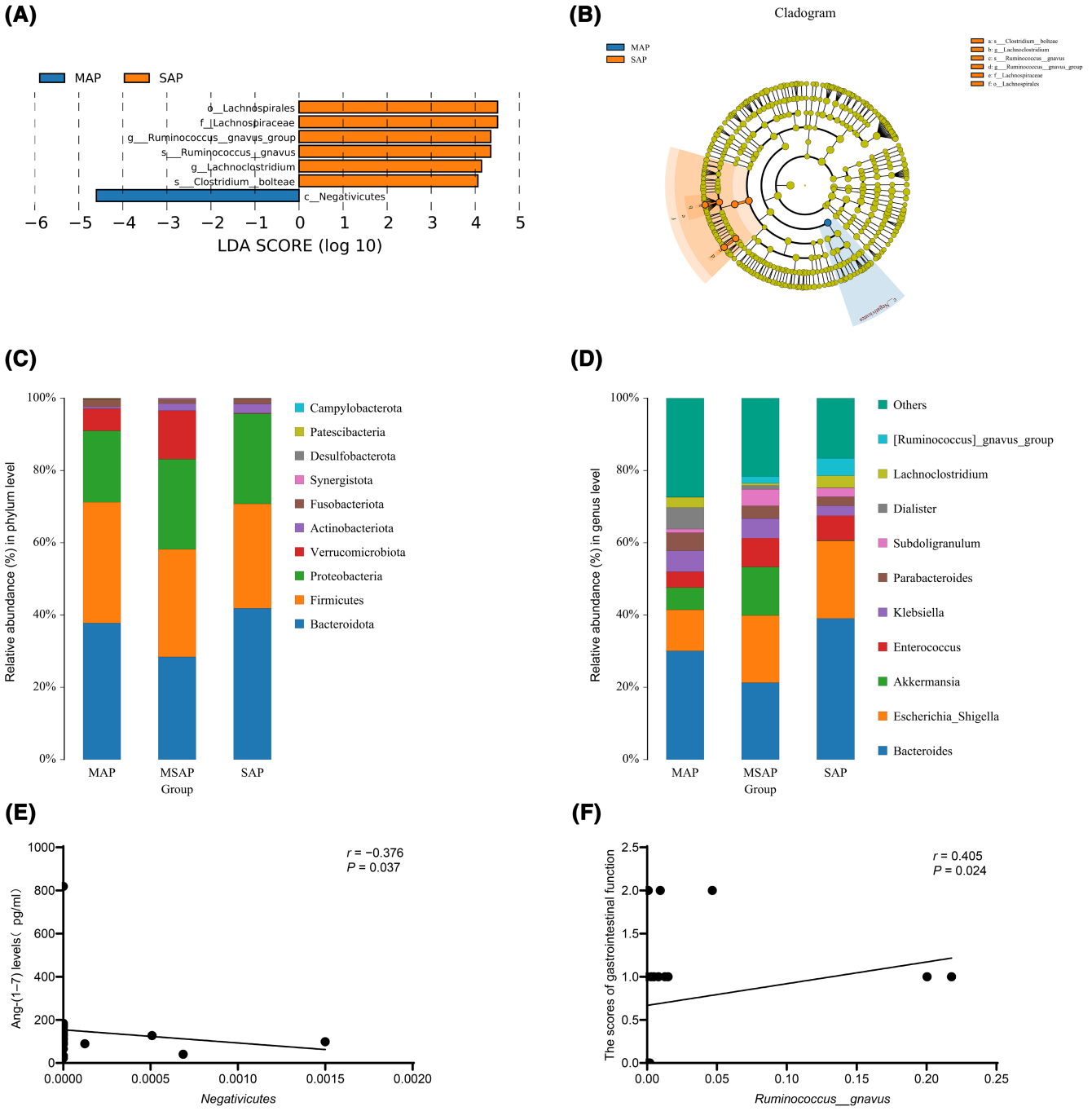

FIGURE 2 Changes in the taxonomic composition of ileum microbial communities at the phylum and genus levels in AP patients. Statistical differences in the levels of biomarkers between the MAP, MSAP, and SAP groups were identified using line discriminant analysis (LDA) effect size (LEfSe) method. Taxa enriched in MAP (Blue) and SAP (Orange) groups are indicated by LDA scores. Only the taxa meeting an LDA significant threshold of four are displayed, and the length of histogram represents the influence of different species (A). Cladogram visualizes the output of LEfSe algorithm. Significantly distinct taxonomic nodes are colored and the branch areas are shaded according to the effect size of the taxa (B). The top 10 bacteria, with maximum abundance of ileum bacteria at the phylum (C) and genus (D) levels. (E) The correlation analysis between *Negativicutes* and serum Ang-(1–7) levels. (F)The correlation analysis between *Ruminococcus gnavus* and gastrointestinal function scores.

also revealed that abundances of inflammation-related genera such as *C. bolteae* and *R. gnavus* were increased in SAP patients compared to MAP and MSAP. Active inflammatory bowel disease is accompanied by an increase in *R. gnavus*. Previous studies have shown a positive correlation between *R. gnavus* and irritable bowel syndrome, Crohn's disease, and other diseases.[25,26] *C. bolteae* may be a vital etiological factor of optic neuromyelitis by molecular

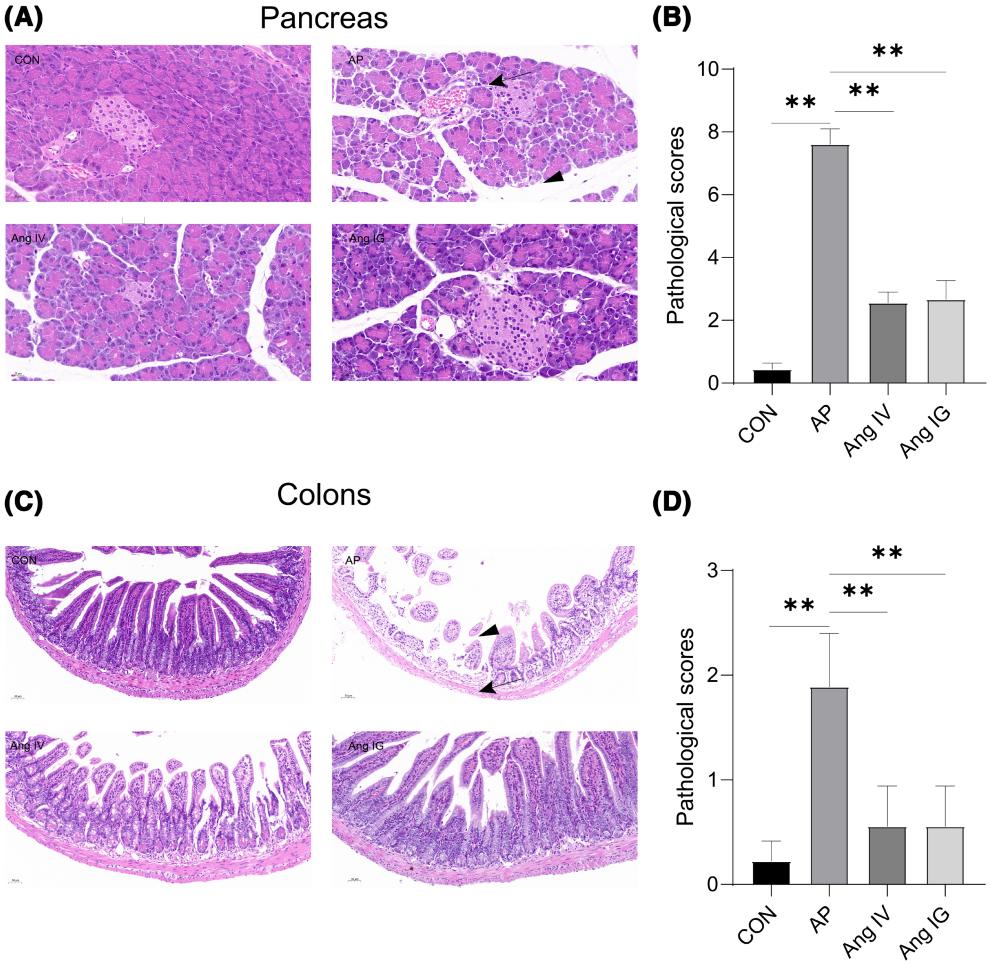

FIGURE 3 Ang-(1–7) treatment protected pancreas and intestine injuries in AP mice. (A) HE staining of pancreas in each group (original magnifcation ×400). Areas of inflammation (arrow) and interlobular edema (arrowhead). Scale bar: 20 μm. (B) Histopathological scores of the pancreas tissues. (C) HE staining of the intestine in each group (original magnifcation ×200). The small intestinal mucosal epithelial cell layers (arrow) and villi (arrowhead). Scale bar: 50 μm. (D) Histopathological scores of the intestine tissues. $n = 3$ for each group. $^{**}p < .01$.

simulation of activation of autoreactive T cells and production of autoantibodies.[27] Thus, we suggested that AP progression decreases the content of SCFA-producing bacteria and increases the content of pathogenic bacteria, resulting in the disruption of the intestinal barrier and the promotion of bacterial translocation.

The study showed that the serum Ang-(1–7) levels of patients were increased with the deterioration of AP, but there was no statistical significance. Our previous study has found that SAP promotes increased serum Ang-(1–7) in mice.[12] Several studies have found intestinal permeability increased in AP patients, and a worsening dysfunction has been found in SAP compared with MAP.[8,28] We found that the gastrointestinal function scores and intestinal permeability indexes (DAO and D-lac) increased with the progression of AP. The correlation analysis was conducted between these indexes and intestinal flora, showing that there was a significant negative correlation between *Negativicutes* and serum Ang-(1–7) levels. There was a significant positive correlation between *R. gnavus* and gastrointestinal function scores. Based on the above results, we inferred that intestinal injury and disease severity may worsen with the disordered intestinal microbiota in AP. Ang-(1–7) levels were associated with changes in the microbiota. Moreover, Ang-(1–7) is a potential target for regulating intestinal microbiota.

Our data identified that Ang-(1–7) attenuated intestinal injuries in AP mice, but the effect of Ang-(1–7) on intestinal microbiota remains unclear. The intestinal microbiota imbalance appears in AP patients and mice.[6,7] In the present study, dramatic alterations were viewed in microbial profiles between the CON and AP mice, and most of these alterations were attenuated by Ang-(1–7). A study reported that there was a higher proportion of harmful bacteria, specifically *Escherichia–Shigella* and *Enterococcus,* in the SAP mice 12 h after AP induction.[29]

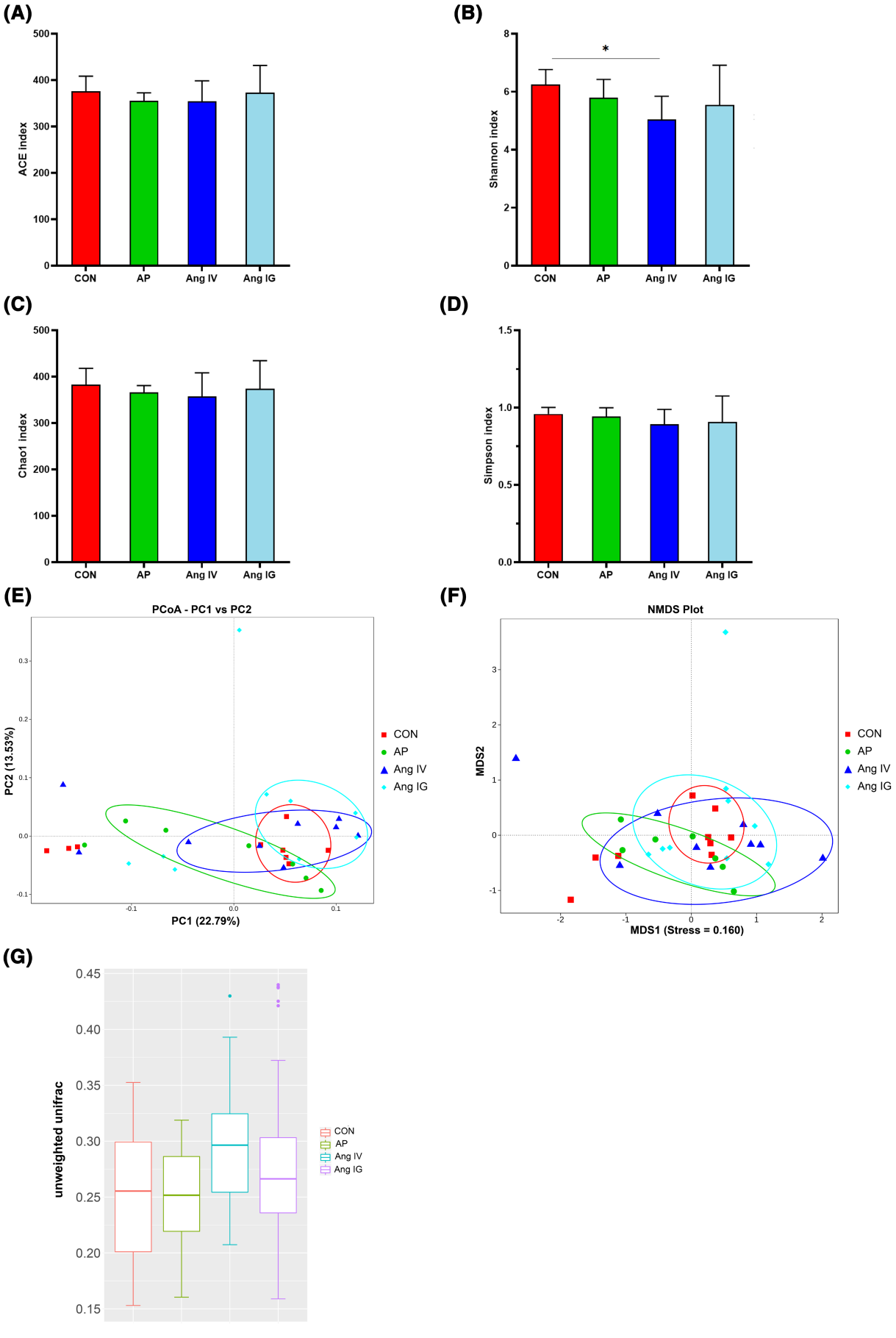

FIGURE 4 The effects of Ang-(1–7) on alpha and beta diversity of gut microbiota in AP mice. Analysis of gut microbial diversity was performed on the basis of 16S rDNA sequencing. (A) ACE index. (B) Shannon index. (C) Chao1 index. (D) Simpson index. Bacterial community compositional similarity was evaluated by beta diversity. PCoA (E) and NMDS plots based on Jaccard dissimilarity (F) are presented. Anosim was used to detect differences between the groups (G). $n = 7–9$ for each group. $^*p < .05$.

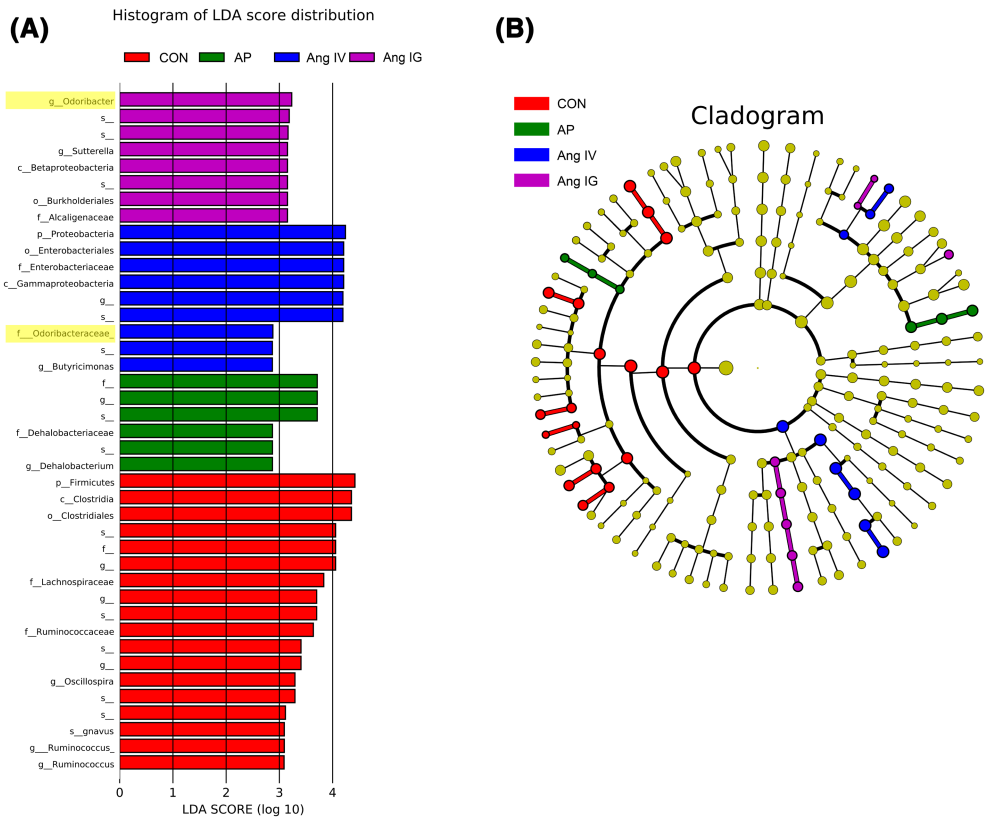

FIGURE 5 Ang-(1–7) supplementation modulated the intestinal microbiota composition in AP mice. Statistical differences in the levels of biomarkers between the control, AP, Ang IV, and Ang IG groups were identified using the LEfSe method. Taxa enriched in control (Red), AP (Green), Ang IV (Blue), and Ang IG (Purple) groups are indicated by LDA scores. Only the taxa meeting an LDA significant threshold of two are displayed, and the length of histogram represents the influence of different species (A). Cladogram visualizes the output of LEfSe algorithm. Significantly distinct taxonomic nodes are colored and the branch areas are shaded according to the effect size of the taxa (B). $n = 7–9$ for each group.

Consistent with these studies, our results confirmed that intestinal microbiota dysbiosis occurred at an early stage (12 h) in AP mice. The results from LEfSe showed that AP reduced the content of *Oscillospira and Lachnospiraceae* and increased the content of *Dehalobacterium* compared with the CON group. Our results were consistent in AP patients and mice, suggesting that AP may lead to a decrease in SCFA-producing bacteria. *Oscillospira and Lachnospiraceae,* known for producing SCFAs, are important to alleviate intestinal injury and intestinal gut barrier.[30,31] Recent studies identified that *Dehalobacterium* is a sensitive index of postoperative cognitive impairment in aged mice and the probiotic treatment improved cognitive score with a decrease in *Dehalobacterium* in middle-aged and older adults.[32,33] The results from LEfSe analysis showed that *Odoribacter* and *Sutterella* genera were enriched in the Ang-(1–7) IG group, whereas the *Odoribacteraceae* and *Butyricimonas* genera were enriched in the Ang-(1–7) IV group, which indicate that Ang-(1–7) could restore gut dysbiosis in AP mice. The genera *Odoribacter* include some species that have been related to SCFA production.[34] The key enzymes for the synthesis of secondary bile acids (5AR and 3β-HSDH) are found in the genomes of *Odoribacter*.[35] Thus, the *Odoribacter* strains produce isoallolithocholic acid and related secondary bile acids, exerting antimicrobial effects against pathogens and maintaining intestinal homeostasis.[35] The content of the butyrate-producing genus *Butyricimonas* is negatively correlated with inflammatory bowel diseases.[36] Consistently, Buford et al. have found that Ang-(1–7) delivered orally

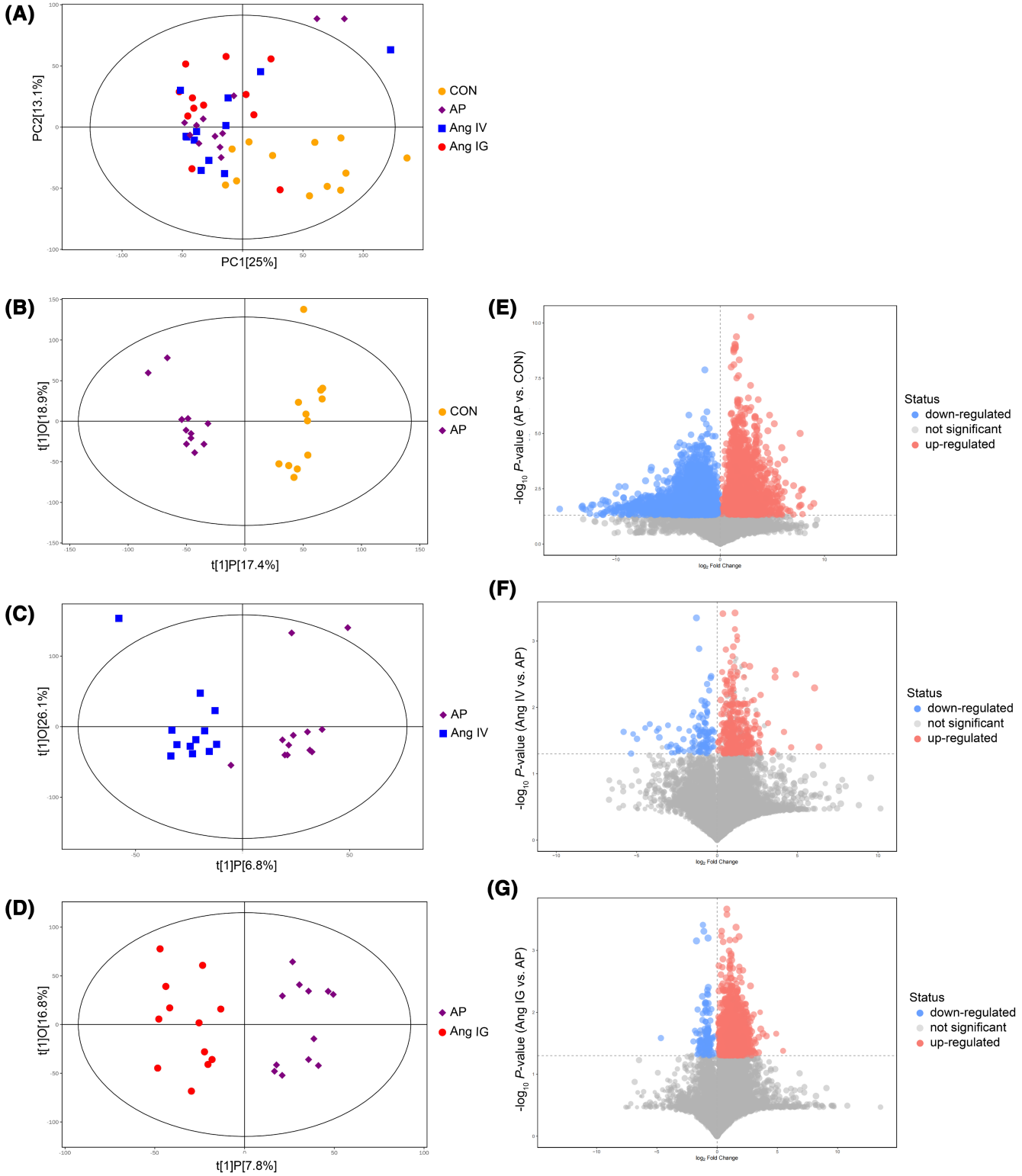

FIGURE 6 The effects of Ang-(1–7) on fecal metabolomic profiles in AP mice. Score scatter plot for the principal component analysis (PCA) model indicated that most of the samples are in 95% Hotelling's T-squared ellipse. The abscissa and ordinate represent the scores of the first and second principal components, respectively. The color and shape of scatter points represent the experimental grouping of samples (A). The orthogonal variables irrelevant to the categorical variables in the metab_x0002_olites were excluded through orthogonal projections to latent structures discriminant analysis (OPLS-DA). The abscissa represents the predicted score of the first principal component, whereas the ordinate represents the score of the orthogonal principal component (B–D). (E) Volcano plot for group AP vs. CON. (F) Volcano plot for group Ang IV vs. AP. (G) Volcano plot for group Ang IG vs. AP. Red dots represent upregulated metabolites and blue dots represent downregulated metabolites. $n = 12$ for each group.

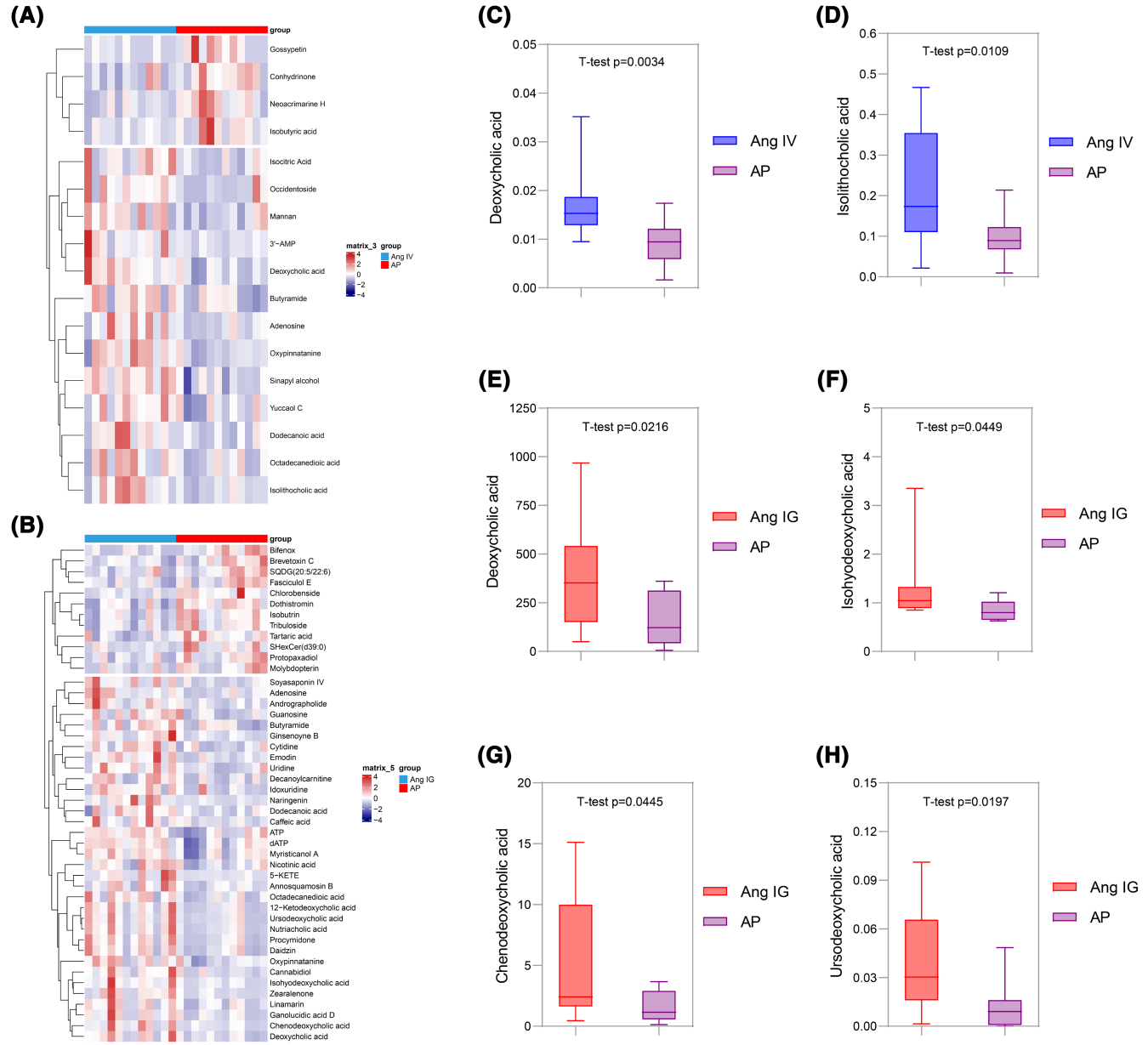

FIGURE 7 Ang-(1–7) treatment affected the abundance bile acids. Difference in fecal metabolomic profiles abundance between the groups. An average heat map of the hierarchical clustering analysis for the two groups is presented. Abscissas represent different experimental groups, ordinates represent different metabolites, and different colors represent the relative expression of metabolites at the corresponding position. (A) Heat map for group Ang IV vs. AP. (B) Heat map for group Ang IG vs. AP. (C and D) The abundances of deoxycholic acid and isolithocholic acid between the Ang IV and AP groups. (E–H) The abundances of deoxycholic acid, isohyodeoxycholic acid, chenodeoxycholic acid, and ursodeoxycholic acid between the Ang IG and AP groups. $n = 12$ for each group.

via probiotic increases the content of SCFA-producing bacteria in older rats.[10] Therefore, we hypothesized that administration with Ang-(1–7) ameliorates intestinal dysfunction in AP mice by increasing SCFAs and secondary bile acid-producing bacteria. Furthermore, the genera *Odoribacter* and *Odoribacteraceae* are promising bacterial targets for regulating AP.

A previous study discovered the beneficial effects of Ang-(1–7) in ameliorating the metabolic perturbations associated with cardiac fibroblast activation in vitro.[37] Nevertheless, there is no research to explore the effect of Ang-(1–7) on fecal metabolites in vivo. For the first time, we reported that Ang-(1–7) reshapes the fecal metabolites in AP. The oral administration of Ang-(1–7) reversed the decrease of emodin and naringenin in AP mice, which may be directly related to intestinal function improvement. In the SAP mice, emodin was found to inhibit apoptotic pathways and modulate immune responses for maintaining the intestinal barrier.[38] Yan et al. discovered that naringenin exerts protective effects on intestinal injury of CAE-induced pancreatitis by

the inactivation of NLRP3 inflammasome.[39] Surprising, we found that Ang-(1–7) had the ability to increase the production of bile acids, especially secondary bile acids. Zhu et al. report serum chenodeoxycholic acid levels were significantly decreased in AP mice, consistent with the trend in humans. Chenodeoxycholic acid supplementation significantly increases the downstream secondary bile acids and protects pancreatic necrosis both in vitro and *vivo*.[40] The secondary bile acids ameliorated pancreatic damage depending on their hydrophobicity in AP mice.[41] These results suggested that the supplementation of bile acids might constitute a potential therapeutic method in AP. The DA Score also illustrated that oral administration of Ang-(1–7) upregulated the bile secretion pathway. Collectively, our results indicated that Ang-(1–7) treatment could regulate the composition of intestinal microbiota and enhance the production of bile acids to protect the intestinal barrier. The effects of the injection and oral administration were no different. However, the oral administration of Ang-(1–7) is more promising for clinical use.

One limitation of this study is that it was conducted at a single center. Another limitation is that the dietary habits of patients were not well documented. To compensate, the participants in our survey all lived in Beijing. The study minimizes the interference of dietary habits in different regions with intestinal microbiota.

In summary, AP resulted in a decrease in SCFA-producing bacteria and an increase in pathogenic bacteria in the intestine. Ang-(1–7) protected against AP by reversing gut microbiota dysbiosis, and modulating the fecal metabolites. These results suggested that oral administration of Ang-(1–7) could be a potential therapeutic agent for AP.

AUTHOR CONTRIBUTIONS

Ruru Gu: Conceptualization (equal); data curation (equal); formal analysis (equal); investigation (equal); methodology (equal); project administration (equal); validation (lead); visualization (lead); writing—original draft (lead). **Hongtao Wei:** Conceptualization (equal); data curation (equal); formal analysis (equal); investigation (equal); project administration (equal); validation (supporting); writing—original draft (supporting). **Tianyu Cui:** Methodology (equal); software (equal); visualization (supporting). **Guoxing Wang:** Funding acquisition (equal); resources (supporting); supervision (equal). **Yingyi Luan:** Software (equal); writing—review & editing (equal). **Ruixia Liu:** Software (equal); writing—review & editing (equal). **Chenghong Yin:** Funding acquisition (equal); resources (lead); supervision (Equal); writing—review & editing (equal).

ACKNOWLEDGMENTS

None.

FUNDING INFORMATION

None.

DISCLOSURES

The authors declare that they have no conflict of interest.

DATA AVAILABILITY STATEMENT

Sequence data are available in the NCBI database under BioProject accession number PRJNA936670.

ORCID

Ruru Gu https://orcid.org/0000-0003-0096-3870
Hongtao Wei https://orcid.org/0000-0001-7394-7447
Tianyu Cui https://orcid.org/0000-0003-4094-4703
Guoxing Wang https://orcid.org/0000-0001-9592-4545
Yingyi Luan https://orcid.org/0000-0002-6986-1701
Ruixia Liu https://orcid.org/0000-0001-5835-4424
Chenghong Yin https://orcid.org/0000-0002-2503-3285

REFERENCES

1. Petrov MS, Yadav D. Global epidemiology and holistic prevention of pancreatitis. *Nat Rev Gastroenterol Hepatol*. 2019;16(3):175-184.
2. Boxhoorn L, Voermans RP, Bouwense SA, et al. Acute pancreatitis. *Lancet*. 2020;396(10252):726-734.
3. Fishman JE, Levy G, Alli V, Zheng X, Mole DJ, Deitch EA. The intestinal mucus layer is a critical component of the gut barrier that is damaged during acute pancreatitis. *Shock*. 2014;42(3):264-270.
4. Ammori BJ. Role of the gut in the course of severe acute pancreatitis. *Pancreas*. 2003;26(2):122-129.
5. Agarwala R, Rana SS, Sharma R, Kang M, Gorsi U, Gupta R. Gastrointestinal failure is a predictor of poor outcome in patients with acute pancreatitis. *Dig Dis Sci*. 2020;65(8):2419-2426.
6. Zhu Y, He C, Li X, et al. Gut microbiota dysbiosis worsens the severity of acute pancreatitis in patients and mice. *J Gastroenterol*. 2019;54(4):347-358.
7. Chen J, Huang C, Wang J, et al. Dysbiosis of intestinal microbiota and decrease in paneth cell antimicrobial peptide level during acute necrotizing pancreatitis in rats. *PLoS One*. 2017;12(4):e0176583.
8. Besselink MG, van Santvoort HC, Renooij W, et al. Intestinal barrier dysfunction in a randomized trial of a specific probiotic composition in acute pancreatitis. *Ann Surg*. 2009;250(5):712-719.
9. Karnik SS, Singh KD, Tirupula K, Unal H. Significance of angiotensin 1-7 coupling with MAS1 receptor and other GPCRs to the renin-angiotensin system: IUPHAR review 22. *Br J Pharmacol*. 2017;174(9):737-753.
10. Buford TW, Sun Y, Roberts LM, et al. Angiotensin (1-7) delivered orally via probiotic, but not subcutaneously, benefits the gut-brain axis in older rats. *Geroscience*. 2020;42(5):1307-1321.
11. Machado A, Oliveira JR, Lelis DF, et al. Oral angiotensin-(1-7) peptide modulates intestinal microbiota improving metabolic profile in obese mice. *Protein Pept Lett*. 2021;28(10):1127-1137.
12. Wang Y, Wang J, Liu R, et al. Severe acute pancreatitis is associated with upregulation of the ACE2-angiotensin-(1-7)-mas axis and promotes increased circulating angiotensin-(1-7). *Pancreatology*. 2012;12(5):451-457.

13. Gu R, Cui T, Guo Y, et al. Angiotensin-(1-7) ameliorates intestinal barrier dysfunction by activating the Keap1/Nrf2/HO-1 signaling pathway in acute pancreatitis. *Mol Biol Rep*. 2023;50(7):5991-6003.
14. Banks PA, Bollen TL, Dervenis C, et al. Classification of acute pancreatitis—2012: revision of the Atlanta classification and definitions by international consensus. *Gut*. 2013;62(1):102-111.
15. Schmidt J, Lewandrowsi K, Warshaw AL, Compton CC, Rattner DW. Morphometric characteristics and homogeneity of a new model of acute pancreatitis in the rat. *Int J Pancreatol*. 1992;12(1):41-51.
16. Chiu CJ, McArdle AH, Brown R, Scott HJ, Gurd FN. Intestinal mucosal lesion in low-flow states. I. A morphological, hemodynamic, and metabolic reappraisal. *Arch Surg*. 1970;101(4):478-483.
17. Wang Z, Guo M, Li J, et al. Composition and functional profiles of gut microbiota reflect the treatment stage, severity, and etiology of acute pancreatitis. *Microbiol Spectr*. 2023;11(5):e0082923.
18. Wang L, Zhang W, Dai S, Gao Y, Zhu C, Yu Y. Correlation between the gut microbiota characteristics of hosts with severe acute pancreatitis and secondary intra-abdominal infection. *Front Med (Lausanne)*. 2024;11:1409409.
19. Penalva JC, Martínez J, Laveda R, et al. A study of intestinal permeability in relation to the inflammatory response and plasma endocab IgM levels in patients with acute pancreatitis. *J Clin Gastroenterol*. 2004;38(6):512-517.
20. Dai X, Chen L, Liu M, et al. Effect of 6-Methoxybenzoxazolinone on the Cecal microbiota of adult male Brandt's vole. *Front Microbiol*. 2022;13:847073.
21. Vargas JE, Andrés S, Snelling TJ, et al. Effect of sunflower and marine oils on ruminal microbiota, in vitro fermentation and digesta fatty acid profile. *Front Microbiol*. 2017;8:1124.
22. Wong JM, de Souza R, Kendall CW, Emam A, Jenkins DJ. Colonic health: fermentation and short chain fatty acids. *J Clin Gastroenterol*. 2006;40(3):235-243.
23. Tedelind S, Westberg F, Kjerrulf M, Vidal A. Anti-inflammatory properties of the short-chain fatty acids acetate and propionate: a study with relevance to inflammatory bowel disease. *World J Gastroenterol*. 2007;13(20):2826-2832.
24. Kelly CJ, Zheng L, Campbell EL, et al. Crosstalk between microbiota-derived short-chain fatty acids and intestinal epithelial HIF augments tissue barrier function. *Cell Host Microbe*. 2015;17(5):662-671.
25. Henke MT, Kenny DJ, Cassilly CD, Vlamakis H, Xavier RJ, Clardy J. *Ruminococcus gnavus*, a member of the human gut microbiome associated with Crohn's disease, produces an inflammatory polysaccharide. *Proc Natl Acad Sci USA*. 2019;116(26):12672-12677.
26. Baumgartner M, Lang M, Holley H, et al. Mucosal biofilms are an endoscopic feature of irritable bowel syndrome and ulcerative colitis. *Gastroenterology*. 2021;161(4):1245-1256.e20.
27. Pandit L, Cox LM, Malli C, et al. *Clostridium bolteae* is elevated in neuromyelitis optica spectrum disorder in India and shares sequence similarity with AQP4. *Neurol Neuroimmunol Neuroinflamm*. 2020;8(1):e907.
28. Liu H, Li W, Wang X, Li J, Yu W. Early gut mucosal dysfunction in patients with acute pancreatitis. *Pancreas*. 2008;36(2):192-196.
29. Mei QX, Hu JH, Huang ZH, et al. Pretreatment with chitosan oligosaccharides attenuate experimental severe acute pancreatitis via inhibiting oxidative stress and modulating intestinal homeostasis. *Acta Pharmacol Sin*. 2021;42(6):942-953.
30. Chen SY, Zhou QY, Chen L, Liao X, Li R, Xie T. The Aurantii fructus Immaturus flavonoid extract alleviates inflammation and modulate gut microbiota in DSS-induced colitis mice. *Front Nutr*. 2022;9:1013899.
31. Ma L, Ni Y, Wang Z, et al. Spermidine improves gut barrier integrity and gut microbiota function in diet-induced obese mice. *Gut Microbes*. 2020;12(1):1-19.
32. Zhan G, Hua D, Huang N, et al. Anesthesia and surgery induce cognitive dysfunction in elderly male mice: the role of gut microbiota. *Aging (Albany NY)*. 2019;11(6):1778-1790.
33. Aljumaah MR, Bhatia U, Roach J, Gunstad J, Azcarate Peril MA. The gut microbiome, mild cognitive impairment, and probiotics: a randomized clinical trial in middle-aged and older adults. *Clin Nutr*. 2022;41(11):2565-2576.
34. Li H, Cao W, Xie J, et al. α-D-1,6-glucan from Castanea mollissima Blume alleviates dextran sulfate sodium-induced colitis in vivo. *Carbohydr Polym*. 2022;289:119410.
35. Sato Y, Atarashi K, Plichta DR, et al. Novel bile acid biosynthetic pathways are enriched in the microbiome of centenarians. *Nature*. 2021;599(7885):458-464.
36. Takahashi K, Nishida A, Fujimoto T, et al. Reduced abundance of butyrate-producing bacteria species in the fecal microbial Community in Crohn's disease [published correction appears in digestion. 2016;93(2):174]. *Digestion*. 2016;93(1):59.
37. Chen YL, Fan J, Cao L, et al. Unique mechanistic insights into the beneficial effects of angiotensin-(1-7) on the prevention of cardiac fibrosis: a metabolomic analysis of primary cardiac fibroblasts. *Exp Cell Res*. 2019;378(2):158-170.
38. Zhou Q, Xiang H, Liu H, et al. Emodin alleviates intestinal barrier dysfunction by inhibiting apoptosis and regulating the immune response in severe acute pancreatitis. *Pancreas*. 2021;50(8):1202-1211.
39. Yan X, Lin T, Zhu Q, Zhang Y, Song Z, Pan X. Naringenin protects against acute pancreatitis-associated intestinal injury by inhibiting NLRP3 inflammasome activation via AhR signaling [published correction appears in *Front Pharmacol*. 2023;14:1295494]. *Front Pharmacol*. 2023;14:1090261.
40. Zhu Q, Yuan C, Dong X, et al. Bile acid metabolomics identifies chenodeoxycholic acid as a therapeutic agent for pancreatic necrosis. *Cell Rep Med*. 2023;4(12):101304.
41. Tran QT, Sendler M, Wiese ML, et al. Systemic bile acids affect the severity of acute pancreatitis in mice depending on their hydrophobicity and the disease pathogenesis. *Int J Mol Sci*. 2022;23(21):13592.

SUPPORTING INFORMATION

Additional supporting information can be found online in the Supporting Information section at the end of this article.

How to cite this article: Gu R, Wei H, Cui T, et al. Angiotensin-(1–7) improves intestinal microbiota disturbances and modulates fecal metabolic aberrations in acute pancreatitis. *The FASEB Journal*. 2024;38:e70134. doi:10.1096/fj.202401565RR